Inorganic Chemistry

Article

pubs.acs.org/IC

Salicylimine-Based Fluorescent Chemosensor for Aluminum Ions and Application to Bioimaging

Soojin Kim,[†] Jin Young Noh,[‡] Ka Young Kim,[†] Jin Hoon Kim,[‡] Hee Kyung Kang,[†] Seong-Won Nam,[†] So Hyun Kim,[†] Sungsu Park,*[,†,§] Cheal Kim,*[,‡] and Jinheung Kim*[,†]

[†]Department of Chemistry and Nano Science, Ewha Womans University, Seoul, 120-750, Korea

[‡]Department of Fine Chemistry, Seoul National University of Science and Technology, Seoul, Korea

[§]Mechanobiology Institute, National University of Singapore, Singapore 117411

Supporting Information

ABSTRACT: In this study, an assay to quantify the presence of aluminum ions using a salicylimine-based receptor was developed utilizing turn-on fluorescence enhancement. Upon treatment with aluminum ions, the fluorescence of the sensor was enhanced at 510 nm due to formation of a 1:1 complex between the chemosensor and the aluminum ions at room temperature. As the concentration of Al^{3+} was increased, the fluorescence gradually increased. Other metal ions, such as Na^{+}, Ag^{+}, K^{+}, Ca^{2+}, Mg^{2+}, Hg^{2+}, Mn^{2+}, Co^{2+}, Ni^{2+}, Cu^{2+}, Zn^{2+}, Cd^{2+}, Pb^{2+}, Cr^{3+}, Fe^{3+}, and In^{3+}, had no such significant effect on the fluorescence. In addition, we show that the probe could be used to map intracellular Al^{3+} distribution in live cells by confocal microscopy.

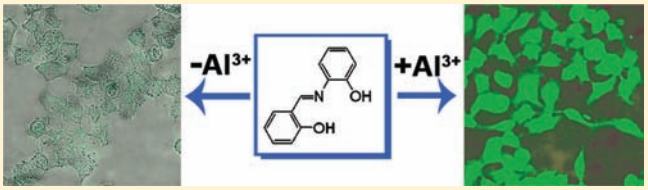

INTRODUCTION

Chemosensors for selective detection of various biologically and environmentally relevant metal ions have recently attracted great attention. The widespread use of aluminum in food additives, aluminum-based pharmaceuticals, and storage/cooking utensils often exposes people to aluminum ions. In addition, frequent use of aluminum foil, vessels, and trays for convenience results in moderate increases in the Al^{3+} concentration in food. After absorption, aluminum ions would be distributed to all tissues in humans and animals and eventually accumulate in the bone. The iron binding protein is known to be the main carrier of Al^{3+} in plasma, and Al^{3+} can enter the brain and reach the placenta and fetus. Aluminum ions may stay for a very long time in various organs and tissues before being excreted through the urine. In addition, aluminum ions have been implicated as a causative factor of Alzheimer's disease and associated with damage to the central nervous system in humans.[1−3] Although trace amounts of aluminum ions are present in the drinking water, low-dose chronic exposure to the ions may cause Alzheimer's disease possibly due to accumulation of oxidative damage induced by the ions.[2] Sensitive bioimaging of Al^{3+} in the cell is a prerequisite for understanding the underlying mechanism about how aluminum ions cause aluminum-induced human diseases including Alzheimer's disease.[3] Thus, detection of Al^{3+} is important to control the concentration levels in the biosphere and minimize direct affects on human health.

In recent years, fluorescent chemosensors have attracted significant interest because of their potential use in medicinal and environmental research. The most commonly employed method used for chemosensor detection is the development of probe molecules that consist of a photon interaction site as a fluorophore and a metal binding site. In the presence of specific metal ions, the fluorophore−receptor communication gets turned on as a result of the binding of the metal ions at the receptor site. Until recently, only a few fluorescent chemosensors have been developed for detection of Al^{3+}.[4−9] Most fluorescent sensors for Al^{3+} have good selectivity, but this approach has several disadvantages including complicated synthetic procedures and poor water solubility. Meanwhile, some Schiff base compounds coordinated to metal ions were reported to have antitumor and antioxidative activities.[10,11] Although many Schiff base derivatives incorporating a fluorescent moiety have been used to detect various metal ions, Schiff base-type Al^{3+} chemosensors are very rare and no examples of water-soluble devices as well as sensors that can be used for cell imaging have been developed.[4] Here, we examine the metal-binding properties of the π-conjugated Schiff base receptor, *o*-phenolsalicylimine (PSI), and report the tridentate ligand PSI as a chemosensor, which exhibits enhanced fluorescence upon binding to Al^{3+} with high selectivity. Possible utilization of PSI as intracellular sensors of Al^{3+} was also examined by confocal fluorescence microscopy.

EXPERIMENTAL SECTION

Materials and Instrumentation. All solvents and reagents (analytical grade and spectroscopic grade) were obtained from Sigma-Aldrich and used as received. Solutions of metal ions were prepared with metal perchlorate salts. ^{1}H NMR spectra were recorded on a Varian 400 spectrometer. Chemical shifts (δ) are reported in

Received: November 15, 2011
Published: March 2, 2012

   dx.doi.org/10.1021/ic2024583 | *Inorg. Chem.* 2012, 51, 3597−3602

ppm, relative to tetramethylsilane $Si(CH_3)_4$. Absorption spectra were recorded at 25 °C using a Perkin-Elmer model Lambda 2S UV/vis spectrometer. Emission spectra were recorded on a Perkin−Elmer LS45 fluorescence spectrometer. Elemental analysis for carbon, nitrogen, and hydrogen was carried out using a vario MACRO (Elemental Analysensysteme, Germany) in the Laboratory Center of the Seoul National University of Science and Technology, Korea. Electrospray ionization mass spectra were collected on a Thermo Finnigan (San Jose, CA, USA) LCQ@ Advantage MAX quadrupole ion trap instrument by infusing samples directly into the source using a manual method. Spray voltage was set at 4.2 kV, and the capillary temperature was at 80 °C.

Synthesis of *o*-Phenolsalicylimine (PSI). A solution of 2-hydroxyaniline (1.42 g, 13 mmol) in absolute ethanol was added to a solution containing 2-hydroxyl-benzaldehyde (1.59 g, 13 mmol) in ethanol. The mixture was refluxed for 1 h under nitrogen. The solution was then cooled to room temperature, and the solvent was evaporated. The orange product was recrystallized from ethanol. The yield of PSI was 91%. ^{1}H NMR (methanol-d_4, 400 MHz) δ: 8.88 (s, 1H), 7.49 (d, 1H), 7.36 (t, 1H), 7.31 (d, 1H), 7.12 (t, 1H), 6.92 (m, 4H). ^{13}C NMR (DMSO-d_6, 100 MHz): δ 161.73, 160.77, 151.18, 134.95, 132.89, 132.37, 128.14, 119.64, 119.60, 119.54, 118.79, 116.74, 116.54 (Supporting Information, Figure S1). FAB MS m/z (M^+): calcd, 213.23; found, 213.22. Anal. Calcd for $C_{13}H_{11}NO_2$ (213.23): C, 73.23; H, 5.20; N, 6.57. Found: C, 73.22; H, 5.22; N, 6.66.

Optical Detection of Al^{3+} Using PSI. The receptor (1.0 μM) was mixed with different concentrations of metal ions in CH_3OH:H_2O (1:1, v/v) in a 1 cm cell. Solutions of metal ions were prepared using nitrate salts. After equilibrium at ambient temperature for 1 min, absorption and fluorescence spectra of the mixtures were measured. Fluorescence spectra were measured at an excitation wavelength of 411 nm.

Methods for Cell Imaging. HeLa cell line (CCL-2, ATCC, Manassas, VA) was cultured in DMEM (Dulbecco's Modified Eagle Medium, Invitrogen, Carlsbad, CA) supplemented with 100 units/mL penicillin (SIGMA), 100 mg/mL streptomycin (SIGMA), and 10% fetal bovine serum (SIGMA) at 37 °C in a humidified incubator. Cells were seeded onto an 18 mm × 8 mm cover glass (Marienfeld, Lauda-Koenigshofen, Germany) at a density of 2×10^5 cells. Cells were then incubated with various concentrations (0.1−100 μM) of $Al(NO_3)_3$ at 37 °C for 4 h. After washing with PBS three times to remove the remaining $Al(NO_3)_3$, the cells were then incubated with 10 μM PSI for 30 min at room temperature. The incubated cells were washed with PBS and mounted onto a glass slide with ClearMount aqueous mounting medium (Invitrogen). Fluorescent images of the mounted cells were obtained using a confocal laser scanning microscope (CLSM LSM510, Carl Zeiss) with 480 nm excitation and 520 nm emission filters at various magnifications (from 200× to 400×).

To fluorescently visualize apoptosis in cells previously exposed to $Al(NO_3)_3$, a TACS 2 TdT-Fluor in situ apoptosis detection kit (Trevigen, Gaithersburg, MD) was used.[12] Cells were incubated and exposed to $Al(NO_3)_3$ as described above. Cells were immersed in TdT buffer (30 mM Trizma base, pH 7.2, 140 mM sodium cacodylate, 1 mM cobalt chloride). TdT labeling solution was then added to cells as suggested by the manufacturer. Cells were then incubated at 37 °C for 60 min. The reaction was terminated by transferring cells to TdT stop buffer (300 mM sodium chloride, 30 mM sodium citrate) for 5 min at room temperature. Cells were rinsed with distilled deionized water (DDW) and incubated with Strep-Fluor solution for 20 min at room temperature. To fluorescently visualize necrosis in cells, the cells previously exposed to $Al(NO_3)_3$ were rinsed with DDW and 1.5 μM propidium iodide (Invitrogen) was added for 15 min. After rinsing with PBS buffer and DDW, cells were prepared for imaging.

RESULTS AND DISCUSSION

The Schiff base probe PSI was synthesized by coupling of 2-hydroxylbenzaldehyde and 2-aminophenol with 91% yield in ethanol (Figure 1 and details in the Experimental Section).

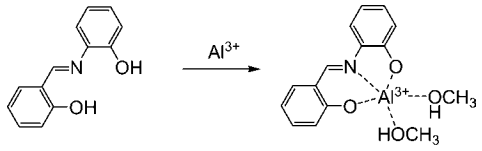

Figure 1. Chemical structures of the receptor PSI and a 1:1 complex of PSI and Al^{3+} in CH_3OH:H_2O.

First, the fluorescence response behavior of PSI was examined upon treatment with various metal ions in methanol−water (1:1, v/v) (Figure 2a). PSI alone showed no

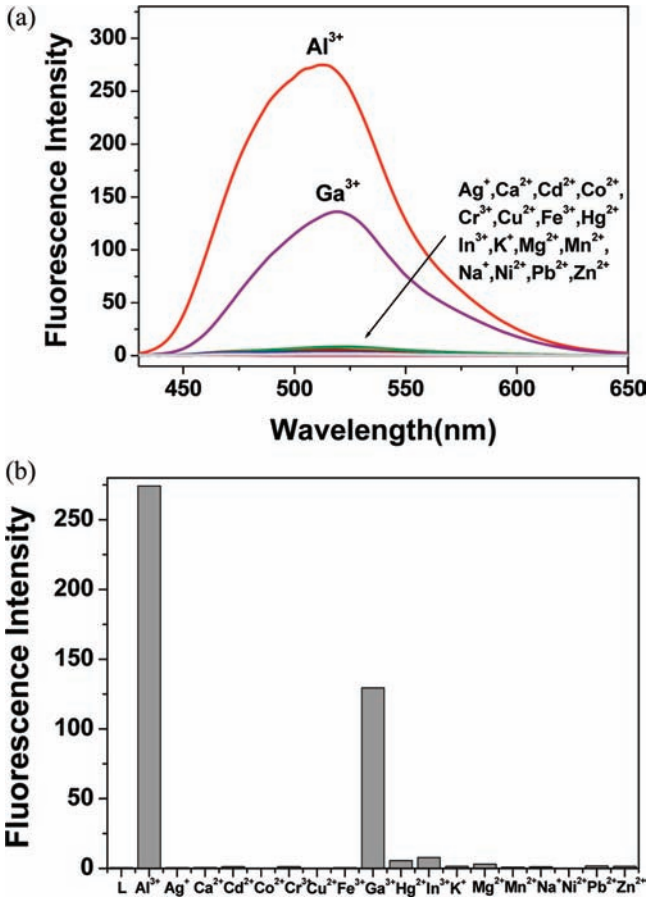

Figure 2. (a) Fluorescence spectra of PSI (1 μM) before and after addition of metal salts (12 μM) of Ag^+, Ca^{2+}, Cd^{2+}, Co^{2+}, Cr^{3+}, Cu^{2+}, Fe^{3+}, Ga^{3+}, Hg^{2+}, In^{3+}, K^+, Mg^{2+}, Mn^{2+}, Na^+, Ni^{2+}, Pb^{2+}, and Zn^{2+} in CH_3OH:H_2O (1:1). (b) Bar graph shows the relative emission intensity of PSI at 510 nm upon treatment with various metal ions.

significant emission after excitation at 411 nm. However, upon addition of Al^{3+}, the fluorescence intensity of PSI increased by a factor of 1000 at a wavelength of 510 nm. In contrast, addition of other relevant metal ions, such as Na^+, Ag^+, K^+, Ca^{2+}, Mg^{2+}, Hg^{2+}, Mn^{2+}, Co^{2+}, Ni^{2+}, Cu^{2+}, Zn^{2+}, Cd^{2+}, Pb^{2+}, Cr^{3+}, Fe^{3+}, and In^{3+}, caused almost no fluorescence increase. Ga^{3+}, which belongs to the same group on the periodic table, also generated a similar fluorescence enhancement centered at 545 nm, but the intensity was significantly lower than with Al^{3+} under the same conditions. It seems that the fluorescence enhancement was derived from the more widespread formation of the π-conjugation system in PSI upon metal binding, and the fluorescence was sensitive to specific metal ions. The selectivity for Al^{3+} with

dx.doi.org/10.1021/ic2024583 | Inorg. Chem. 2012, 51, 3597−3602

1 μM PSI was plotted as a bar graph in Figure 2b. Only Al^{3+} resulted in a pronounced fluorescence enhancement relative to the control ions.

When the PSI sensor was titrated with Al^{3+}, the fluorescence intensity increased up to 13 equiv and then no changes were observed up to 27 equiv (Figure 3). A binding constant (log K_a) of 4.5 was obtained from a nonlinear least-squares fit according to a 1:1 binding stoichiometry (Figure 3b). The close agreement of the experimental data to the theoretical fit indicates that this reaction involves a 1:1 complexation stoichiometry. The log K_a of PSI was within the range 2.9−8.7 of those reported for Al^{3+}-binding sensors.[4−9]

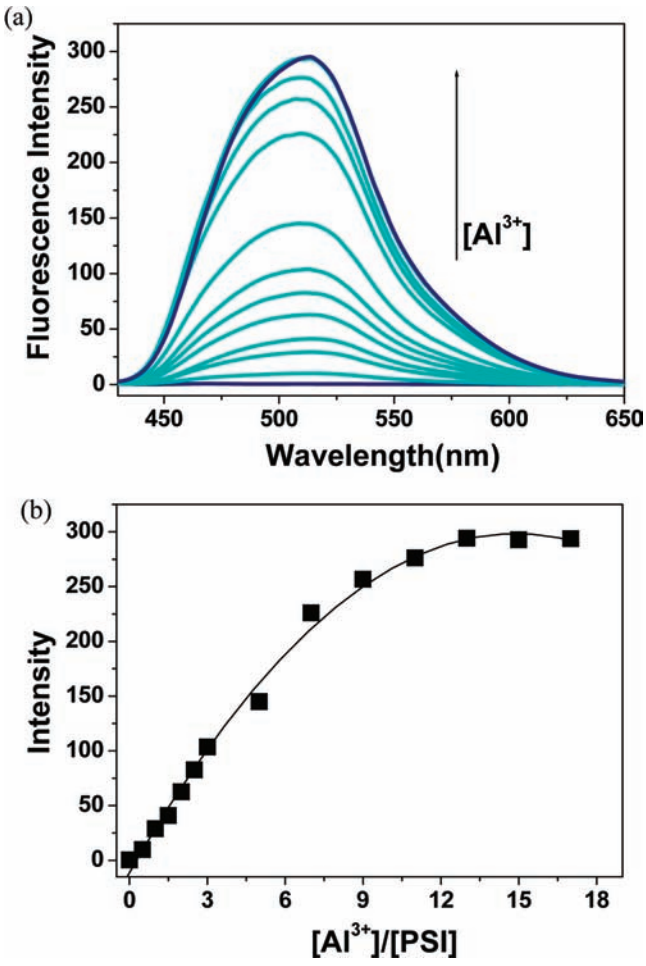

Figure 3. (a) Fluorescence spectra of 1 μM PSI (λ_{ex} = 411 nm) after addition of increasing amounts of Al^{3+} ions (0.5, 1.0, 1.5, 2.0, 2.5, 3.0, 5.0, 7.0, 9.0, 11, 13, 15, 17, and 27 μM) at room temperature. (b) Graph of the fluorescence intensity at 510 nm as a function of Al^{3+} concentration.

We then evaluated changes in the absorbance of PSI upon treatment with Al^{3+} ions. Upon addition of Al^{3+}, the intensity of the absorption bands of PSI at 260 and 345 nm decreased with a concomitant increase in new low-energy peaks at 305 and 415 nm (Figure 4a). Three well-defined isosbestic points at ca. 310, 365, and 460 nm were observed, indicative of a clean conversion of PSI into the PSI−Al^{3+} complex. In addition, the Job's plot, which was based on the changes in absorbance at 415 nm, confirmed formation of a 1:1 complex of Al^{3+} with PSI (Figure 4b). The absorption spectrum of the complex matched the excitation spectrum for formation of the PSI−Al^{3+} complex,

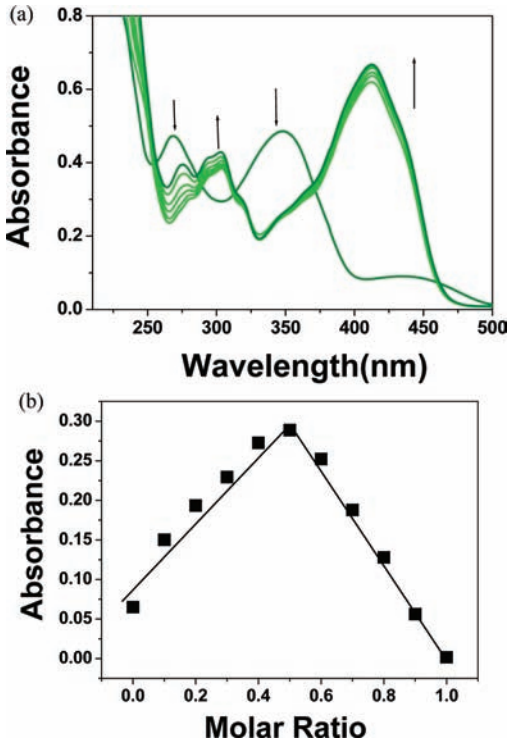

Figure 4. (a) UV−vis spectral changes of 50 μM PSI after addition of aluminum ions (2, 3, 4, 5, 15, and 25 equiv) in CH_3OH−H_2O (1:1). (b) Job's plot for the binding of PSI with Al^{3+}. Absorbance at 415 nm was plotted as a function of the molar ratio $[Al^{3+}]/([PSI] + [Al^{3+}])$.

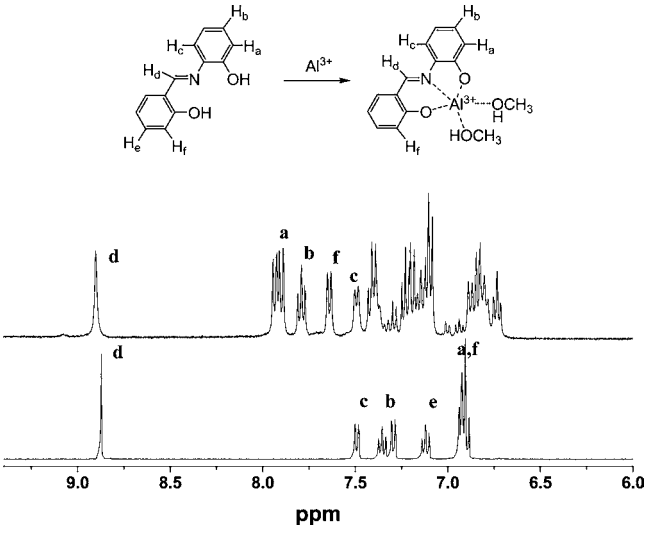

Figure 5. ^{1}H NMR spectra of PSI with and without $Al(ClO_4)_3$ in methanol-d_4: (a) PSI (bottom); (b) PSI with 1 equiv of Al^{3+} (top).

suggesting that the observed absorbance and fluorescence changes resulted from complex formation between PSI and Al^{3+}.

The sensitivity of the aluminum fluorescent probe PSI toward variations in the sample pH was examined by absorption and fluorescence measurements (Supporting Information, Figures S2 and S3). At pH 5.0, 6.0, and 7.0, addition of Al^{3+} to PSI resulted in similar changes in the absorption spectra of the probe. Although the fluorescence intensity of PSI was very weak at low and high pH, PSI showed a meaningful response between pH 4 and 8, while the biologically relevant pH range is

dx.doi.org/10.1021/ic2024583 | Inorg. Chem. 2012, 51, 3597−3602

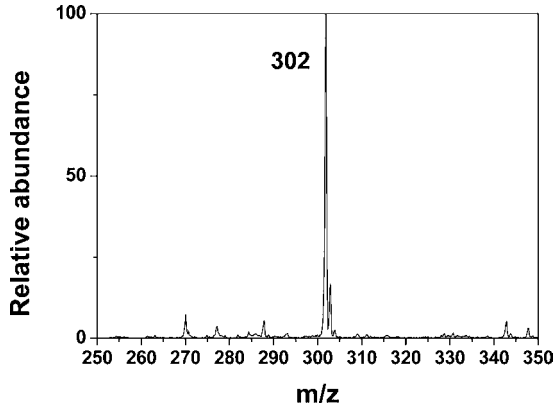

Figure 6. Positive-ion electrospray ionization mass spectrum of PSI upon addition of $Al(NO_3)_3$ (1 equiv) in CH_3OH.

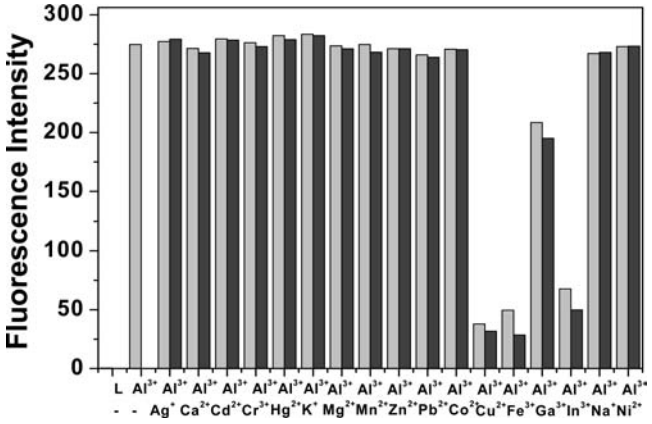

Figure 7. Relative fluorescence of PSI and its complexation with Al^{3+} in the presence of various metal ions. Response of PSI was included as controls. (Left to right) PSI alone (L corresponds to PSI), PSI + Al^{3+}, PSI + Al^{3+} + Ag^{+}, PSI + Al^{3+} + Ca^{2+}, etc. Conditions: 1.0 μM of PSI, 12 equiv of Al^{3+} in the absence and presence of 12 (gray) and 24 equiv (black) of metal ions with (λ_{ex} = 411 nm).

6.0−7.6. These differences may be attributed to decomposition of PSI at a high pH and protonation of the phenol moieties at a low pH.

The binding mode of PSI with Al^{3+} was examined by ^1H NMR in methanol-d_4. Spectra of PSI before and after treatment with 1 equiv of Al^{3+} are shown in Figure 5. Complexation of PSI with Al^{3+} shifted the aromatic proton peaks of phenol to low magnetic field due to the reduction of electron density upon coordination to the metal ion. The H_a, H_b, and H_c protons of the phenol moiety underwent overall large downfield shifts of 1.00, 0.43, and 0.02 ppm, respectively, upon addition of 1.0 equiv of Al^{3+} salt. Similarly, the peak corresponding to the other phenol ring (H_f) was downfield shifted by 0.74 ppm. The imine proton peak (H_d) at 8.82 ppm was also downfield shifted by ca. 0.08 ppm and broadened upon complexation. NMR data demonstrated that adduct formation between Al^{3+} and PSI resulted in these chemical shifts. There were no significant changes with the proton signals upon addition of 2 and 4 equiv of Al^{3+} to PSI (Supporting Information, Figure S4). Electrospray ionization mass spectral analysis also indicated the 1:1 binding stoichiometry of PSI with Al^{3+}. The positive-ion mass spectrum of PSI upon addition of 1 equiv of Al^{3+} exhibited one intense peak at m/z = 302, corresponding to the ion $[Al^{3+} + PSI^{2-} + 2CH_3OH]^+$ (Figure 6). Upon addition of 2 equiv of Al^{3+} to a solution of PSI, no significant changes were observed (Supporting Information, Figure S5).

To examine the selectivity for Al^{3+} in a complex background of potentially competing species, the fluorescence enhancement of PSI with Al^{3+} was investigated in the presence of other metal ions (Figure 7). Except for Fe^{3+}, Cu^{2+}, Ga^{3+}, and In^{3+}, a background of most competing metal ions did not interfere with detection of Al^{3+} by PSI in methanol−H_2O. On the basis of the fluorescence intensities shown in Figure 7, Fe^{3+}, Cu^{2+}, and In^{3+} quenched about 75−80% of the fluorescence obtained with Al^{3+} alone. Interestingly, Ga^{3+} quenched about 40% under the same conditions. These data demonstrate that Fe^{3+}, Cu^{2+}, and In^{3+} interfere with the binding of Al^{3+} to PSI, but the interference from Ga^{3+} was relatively weak.

Subsequent experiments were conducted to test if PSI can be used to fluorescently visualize intracellular Al^{3+}. For this purpose, HeLa cells were first incubated with various concentrations (from 0.1 μM to 1 mM) of $Al(NO_3)_3$ for 4 h and then treated with 10 μM PSI for 30 min before imaging. No fluorescence was observed in cells (Figure 8e) that were not previously exposed to $Al(NO_3)_3$, while strong fluorescence was

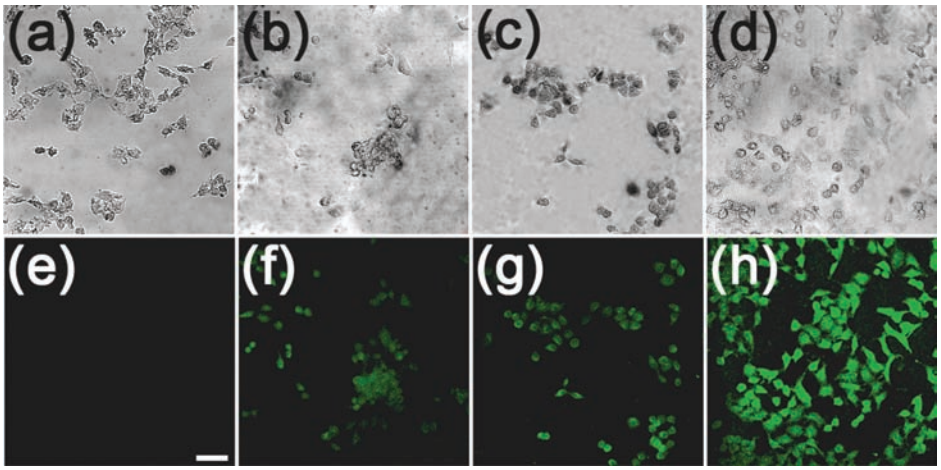

Figure 8. Representative fluorescence images of HeLa cells exposed to various concentrations of $Al(NO_3)_3$ with 10 μM PSI: (a and e) incubated with PSI only; (b and f) incubated with 1 μM $Al(NO_3)_3$ for 4 h and exposed with PSI; (c and g) incubated with 10 μM $Al(NO_3)_3$ for 4 h and exposed with PSI; (d and h) 100 μM $Al(NO_3)_3$ for 4 h and stained with PSI. (a−d) DIC images and (e−h) fluorescent images (excitation = 480 nm, emission = 520 nm LP). Details are found in the Experimental Section. Scale bar represents 50 μm.

dx.doi.org/10.1021/ic2024583 | Inorg. Chem. 2012, 51, 3597−3602

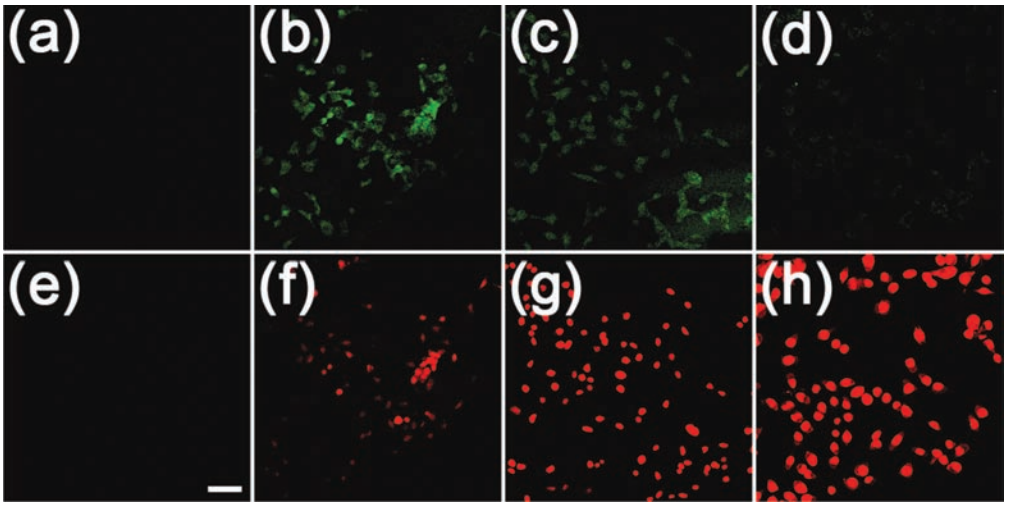

Figure 9. Representative fluorescence images of HeLa cells exposed to various concentrations of Al^{3+} after tunnel assay using a TACS 2 TdT-Fluor in situ apoptosis detection kit and incubation with 1.5 μM propidium iodide: (a and e) cells were not incubated with $Al(NO_3)_3$; (b and f) cells incubated with 1 μM $Al(NO_3)_3$ for 4 h; (c and g) 10 μM $Al(NO_3)_3$ for 4 h; (d and h) 100 μM $Al(NO_3)_3$ for 4 h. (a–d) Fluorescent images of apoptotic cells (excitation = 480 nm, emission = 520 nm long pass) with a TACS 2 TdT-Fluor in situ apoptosis detection kit, and (e–h) fluorescent images of necrotic cells (excitation = 540 nm, emission = 590 nm long pass) with 1.5 μM propidium iodide. Details are found in the Experimental Section. Scale bar represents 50 μm.

observed in cells (Figure 8f–h) exposed to $Al(NO_3)_3$ at different concentrations (1–100 μM). Cells that were exposed to 0.1 μM $Al(NO_3)_3$ displayed negligible fluorescence (data not shown). These results demonstrate that the probe is permeable to cells, binds to intracellular Al^{3+}, and emits fluorescent light upon binding to the metal ion. PSI is highly suitable for determining the exposure level of cells to $Al(NO_3)_3$.

The probe was further used to determine the concentration of $Al(NO_3)_3$ causing cytotoxicity. For this application, a TACS 2 TdT-Fluor in situ apoptosis detection kit and propidium iodide were used to visualize apoptosis and necrosis in cells, respectively. Neither apoptosis nor necrosis fluorescence was observed in the cells that were not exposed to $Al(NO_3)_3$ as shown in Figure 9a and 9e. Cells at 1 μM $Al(NO_3)_3$ (Figure 9b) displayed the strongest apoptosis fluorescence, and apoptosis fluorescence in cells diminished as the concentration of $Al(NO_3)_3$ was increased to 10 and 100 μM, as shown in Figure 9c and 9d, respectively. In contrast with the apoptosis staining results (Figure 9b–d), cells at 1 μM $Al(NO_3)_3$ (Figure 9f) displayed the weakest necrosis fluorescence, and necrosis fluorescence in cells became stronger as the concentration of $Al(NO_3)_3$ was increased to 10 and 100 μM, as shown in Figure 9g and 9h, respectively. On the basis of these results, it is suggested that cytotoxic damages depend on the intracellular level of Al^{3+}.

In conclusion, we developed a turn-on fluorescence method to detect Al^{3+} using a simple salicylimine-based chemosensor with high selectivity in methanol–water. In our assay, Al^{3+} could selectively participate in complex formation with the receptor, which resulted in a color change and fluorescence enhancement. We have also shown that this PSI chemosensor can be applied to living cell imaging to detect and measure the distribution of intracellular Al^{3+}.

■ ASSOCIATED CONTENT

Ⓢ Supporting Information

^{13}C NMR spectrum of PSI, additional UV–visible and fluorescence spectra, ^{1}H NMR spectra of PSI, and ESI mass spectrum. This material is available free of charge via the Internet at http://pubs.acs.org.

■ AUTHOR INFORMATION

Corresponding Author

*Phone: +82-2-3277-4453. Fax: +82-2-3277-3419. E-mail: jinheung@ewha.ac.kr (J.K.); nanopark@ewha.ac.kr (S.P.); chealkim@snut.ac.kr (C.K.).

Notes

The authors declare no competing financial interest.

■ ACKNOWLEDGMENTS

This work was supported by the National Research Foundation of Korea Grant funded by the Korea Government (2010-0009525), Korea Science & Engineering Foundation (2009-0074066), Converging Research Center Program through the National Research Foundation of Korea (NRF) funded by the Ministry of Education, Science and Technology (2011K000675), and BK21 (to S.L., K.Y.K., and H.K.K.).

■ REFERENCES

(1) Cronan, C. S.; Walker, W. J.; Bloom, P. R. *Nature* **1986**, *324*, 140–143.
(2) Walton, J. R. *J. Inorg. Biochem.* **2007**, *101*, 1275–1284.
(3) (a) Nayak, P. *Environ. Res.* **2002**, *89*, 101–115. (b) Fasman, G. D. *Coord. Chem. Rev.* **1996**, *149*, 125–165.
(4) Park, H. M.; Oh, B. N.; Kim, J. H.; Qiong, W.; Hwang, I. H.; Jung, K.-D.; Kim, C.; Kim, J. *Tetrahedron Lett.* **2011**, *52*, 5581–5584.
(5) (a) Maity, D.; Govindaraju, T. *Chem. Commun.* **2010**, 4499–4501. (b) Maity, D.; Govindaraju, T. *Inorg. Chem.* **2010**, *49*, 7229–7231.
(6) (a) Lohani, C. R.; Kim, J.-M.; Chung, S.-Y.; Yoon, J.; Lee, K.-H. *Analyst.* **2010**, *135*, 2079–2084. (b) Jang, H. O.; Nakamura, K.; Yi, S.-S.; Kim, J. S.; Go, J. R.; Yoon, J. *J. Inclusion Phenom. Macrocycl. Chem.* **2001**, *40*, 313–316.
(7) Ren, J. L.; Zhang, J.; Luo, J. Q.; Pei, X. K.; Jiang, Z. X. *Analyst* **2001**, *126*, 698–702.
(8) Wang, Y.-W.; Yu, M.-X.; Yu, Y.-H.; Bai, Z.-P.; Shen, Z.; Li, F.-Y.; You, X.-Z. *Tetrahedron Lett.* **2009**, *50*, 6169–6172.

(9) Kim, S. H.; Choi, H. S.; Kim, J.; Lee, S. J.; Quang, D. T.; Kim, J. S. *Org. Lett.* **2010**, *12*, 560−563.
(10) Padhye, S.; Kauffman, G. B. *Coord. Chem. Rev.* **1985**, *63*, 4823−4831.
(11) de Silveira, V. C.; Luz, J. S.; Oliveira, C. C.; Graziani, I.; Ciriolo, M. R.; Ferreira, A. M. D. C. *J. Inorg. Biochem.* **2008**, *102*, 1090−1103.
(12) Nam, S. W.; Chen, X.; Lim, J.; Kim, S. H.; Kim, S. T.; Cho, Y. H.; Yoon, J.; Park, S. *PLos One* **2011**, *6*, e21387.